

Summer 6-26-2014

Effective permeability upscaling from heterogenous to homogenous porous media

Mehmet Cicek

University of Oklahoma Norman Campus

Deepak Devegowda

University of Oklahoma Norman Campus

Faruk Civan

University of Oklahoma Norman Campus

Richard Sigal

Las Vegas

Follow this and additional works at: http://dc.engconfintl.org/porous_media_V



Part of the [Materials Science and Engineering Commons](#)

Recommended Citation

Mehmet Cicek, Deepak Devegowda, Faruk Civan, and Richard Sigal, "Effective permeability upscaling from heterogenous to homogenous porous media" in "5th International Conference on Porous Media and Their Applications in Science, Engineering and Industry", Prof. Kambiz Vafai, University of California, Riverside; Prof. Adrian Bejan, Duke University; Prof. Akira Nakayama, Shizuoka University; Prof. Oronzio Manca, Seconda Università degli Studi Napoli Eds, ECI Symposium Series, (2014). http://dc.engconfintl.org/porous_media_V/38

This Conference Proceeding is brought to you for free and open access by the Refereed Proceedings at ECI Digital Archives. It has been accepted for inclusion in 5th International Conference on Porous Media and Their Applications in Science, Engineering and Industry by an authorized administrator of ECI Digital Archives. For more information, please contact franco@bepress.com.

EFFECTIVE PERMEABILITY UPSCALING FROM HETEROGENEOUS TO HOMOGENOUS POROUS MEDIA

Mehmet Cicek, Deepak Devogowda, Faruk Civan
University of Oklahoma, Norman, Oklahoma, 73019, USA

Richard F. Sigal
Las Vegas, NV 89131, USA

ABSTRACT

An effective method to upscale permeability is presented to represent a heterogeneous reservoir with homogeneous permeability and porosity values. As a result, there is no need to deal with dual-porosity or dual-permeability models in reservoir simulations. Thus, the required CPU time for reservoir production and flow simulations is reduced significantly.

INTRODUCTION

The petroleum exploration and production researchers study the rocks and earth at different scales. While well logs measure in feet scale, laboratory tests conclude about inches of rocks, moreover SEM studies have resolutions of nanometers. If every feature in a rock is attributed to a grid block in a flow simulator, any reservoir would require billions of grid blocks and flow equations to solve. This requires extensive amount of CPU time. On the other hand, if large grid blocks can be represented with upscaled properties, the required time will dramatically decrease. Especially in the cases like uncertainty analysis or when reservoir conditions are being updated regularly, the decrease in computing time of repetitive simulations will be significant.

This paper suggests a very practical method to upscale the permeability of a reservoir. By the help of a reservoir modelling program, different heterogeneous reservoir cases are generated and production curves are compared with many homogenized reservoirs, which have prescribed permeability values, using a commercial CFD simulator. Best matches between the generated and homogenized reservoir models point to the upscaled permeability value graphically. Once the rock or reservoir is upscaled, further flow simulation of any purpose will not require dealing with different flow models like dual-porosity and dual-permeability, because the upscaled permeability and porosity values will be valid for every grid block in the rock and a standard single-porosity model will be sufficient. In addition these upscaled values make some flow simulators applicable which only allow for use of a single permeability value for the entire system.

Even though the emphasis of this study will be on petroleum reservoirs, the same method can be used in different fields, such as permeability up-scaling in geothermal reservoirs and chemical or biological waste spreading cases and impermeability up-scaling for dam linings and clays in which nuclear wastes are repositied.

A rock is a cemented stack of different minerals and grains. Mismatches of angular grains create pore spaces. The subsurface oil, gas, and water reside in tight pore spaces with high pressures up to 10000 psia. In addition, post-depositional changes can create some fractures within the rocks. Whenever we stimulate a rock body by completing a wellbore within it, causing a pressure drop; oil, gas, and water move through pore spaces and fractures, and reach the wellbore so that they are produced to the surface. This makes the whole process a porous media flow problem.

Shale is a kind of rock from which petroleum industry has recently started to produce oil and gas with large rates and is commonly known by its high organic content and ultra-low permeability. Thus, the composite of the low-permeable matrix, stimulated or natural fractures, and organics form a highly heterogeneous and anisotropic medium acting as the reservoir. Depending on the causing effect and process conditions, different kinds of fractures may form; and their patterns and permeability values may largely differ from each other. For example gouge-filled fractures reduce permeability perpendicular to the fracture plane and have no effect on parallel to the fracture plane (Nelson, 2001). In this study we employ open fractures, which have very large benefit on permeability along fracture plane with almost no effect normal to the fracture plane. We use open fractures to help petroleum production. The man-made fractures are a very common application.

NOMENCLATURE

c	=	Complex number for desired shape
e	=	Exponential constant
K	=	Permeability
N	=	Number of grid cell
Q	=	Resulting complex number
W	=	Equivalent of each complex number

Z = Complex number for every (x, y) couple in a domain

Greek Symbols

ϕ = Porosity

Subscripts

f = Fracture
h = Homogenized model
m = Matrix
o = Organics
T = Total
x = Property in x-direction
y = Property in y-direction

1 Methodology

According to rock samples of different scales, like outcrops, thin sections and SEM images, organic materials are distributed heterogeneously within inorganic matrix and fractures exist randomly or weakly-ordered in nature. We approach rocks as they are composed of those three sub-elements, which are inorganics, organics and fractures. Reservoir models with orthogonal grid system are built, every grid block correspond to one sub-element and every type of sub-element is modelled in individual layers and superposed for the final model. For fracture layers we implement three different approaches, one random linear model and two random fractal models. For organics layer on the other hand, we use a total random distribution throughout the reservoir. As seen, randomness is the key feature of this study because it is impossible to always have a representative sample from a reservoir. By the help of this randomness, different and extreme cases that are possible to be observed in different samples are achieved. Every step of this realization is automated by a program we coded.

After those three reservoir models are generated, we converted them for applications with the commercial simulator grid. Every grid block on the base models are represented by their location and sub-element type in the simulator. Fractured and heterogeneous/anisotropic base models are estimated by dual porosity model. This model is commonly accepted for shale reservoirs where the matrix permeability is very low and the main flow takes place only in high-permeable fractures. Reservoir pressure changes with respect to time of these three base models are estimated and compared with homogenized models, which have the same total porosity of the base models shared by each grid cell and a single permeability value.

Pressure vs time graphs of different homogenized models are stacked together to have a 3-D graph, where vertical y-axis is pressure in psia, x-axis is time in day and z-axis is the identification number of homogenized model. Because the only difference between homogenized models is the permeability value, the z-axis actually represents the axis of permeability. Base model plots of pressure versus time are also added to the previous 3-D

graph with no change along z-axis. The line along which the base model and the homogenized model surfaces intersect points the representative homogenized models and the upscaled permeability value used for that heterogeneous/anisotropic base model.

1.1 Random Linear Fracture Model

Fractures are modelled grid by grid. As stated by various studies in literature, fractures start to grow from one point and continue in some direction depending on the external and internal factors, such as differential principal stress and anisotropy of the material. Starting point positions are attained randomly but the number of starting points is decided depending on the desired intensity. In every grid block, the program decides in which direction the fracture will go, for this we applied a probability function. We selected the maximum principal stress is in x-direction, thus the fracture will have a tendency to go towards it, but due to some internal factors which are not the issue of this paper the fracture may deflect to positive or negative y-direction.

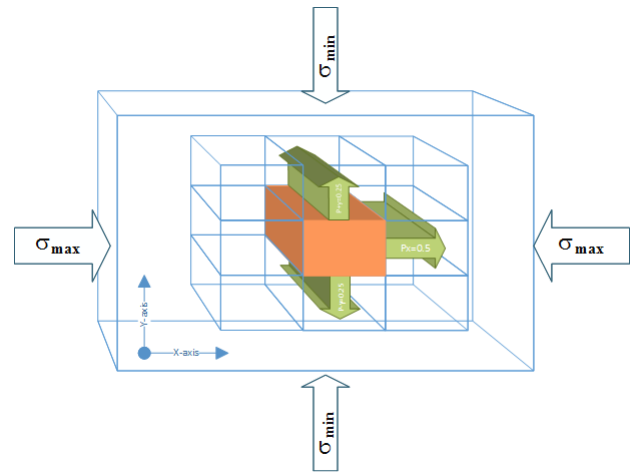


Figure 1: Every grid block decides which direction to propagate

For every grid block, the program also decides how many grid blocks will the fracture keep propagate in a certain direction. This is a property related with the local weaknesses of the rock and the applied force. Because a long distance to propagate includes smaller and many distances, it will be hard to form a small crack and so the probability becomes lower as the fracture gets longer.

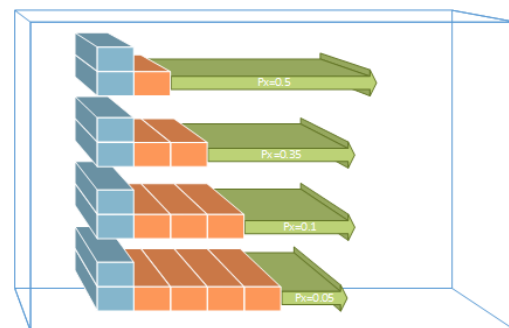


Figure 2: Probability of a longer fracture is lower to form

Total fracture length is another property here to be decided by the program. After a predefined length the fracture terminates but before that length the program also decides whether the fracture will continue to grow or stop growing.

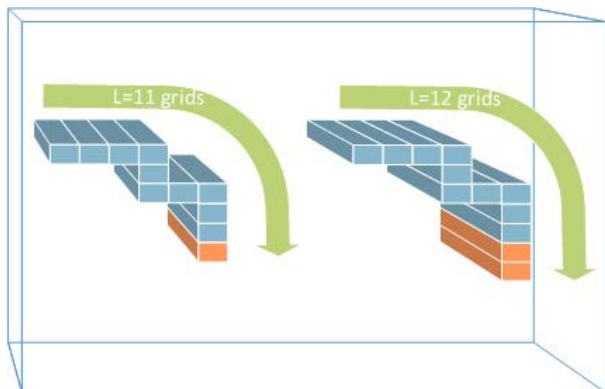


Figure 3: Total length of every fracture is also controlled by probability functions

The resulting random linear fracture model also shows the length of each branch from starting point (head) to tip with color-code. As a fracture length increases its cool-colors (blue, green) turns to warm-colors (yellow, red).

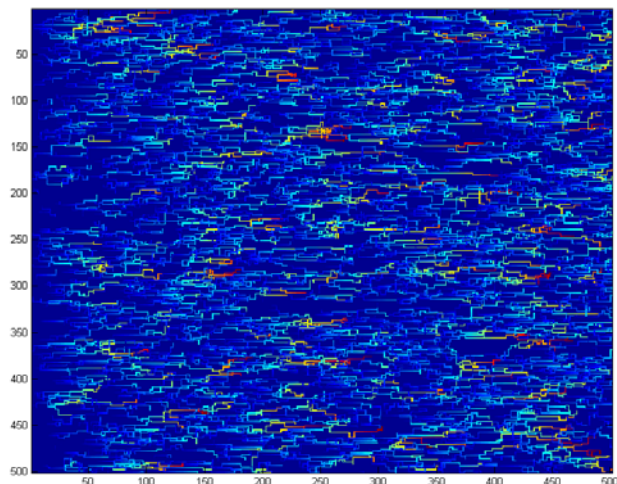


Figure 4: Final "Random Linear Fracture" model

1.2 Fractal Based Random Fracture Models

We implemented two different fractal approaches. In the first, a fracture branch repeats itself in every step starting from the previous branch getting smaller in size. The direction of each new branch is decided by a probability function. As a result we have a tree-like or river-system-like fracture network in which all far branches are actually rooted at the very first starting point.

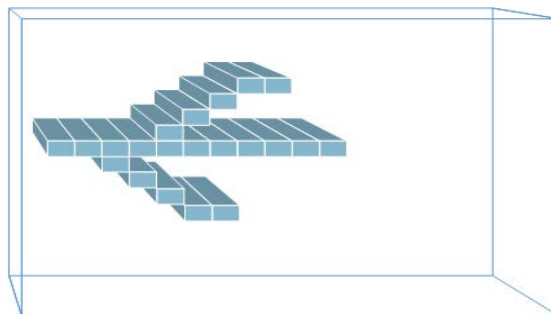


Figure 5: Basis of "Linear Fractal Fracture"

The main motivation for this model is that, after a big outside effect the rock has started to fracture but the effect had diminished and because shales are ductile materials they absorb the energy elastically. As the distance increases from the original starting point the length of the new fracture gets shorter. The color in the final model (Figure 8) also represents the length of the fracture.

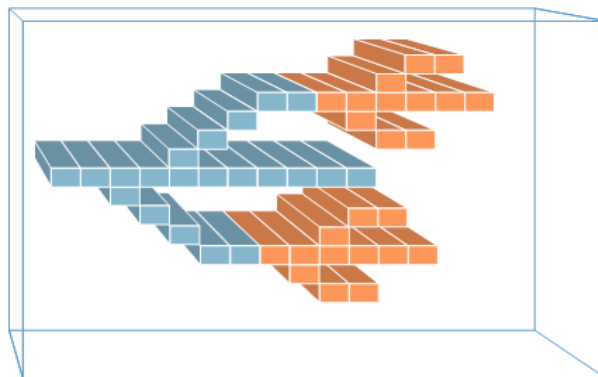


Figure 6: At the second step daughter branch will have the same pattern with a smaller size.

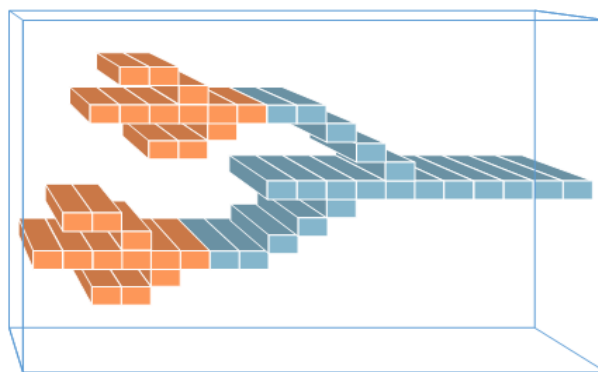


Figure 7: Direction of each branch is controlled by probability functions.

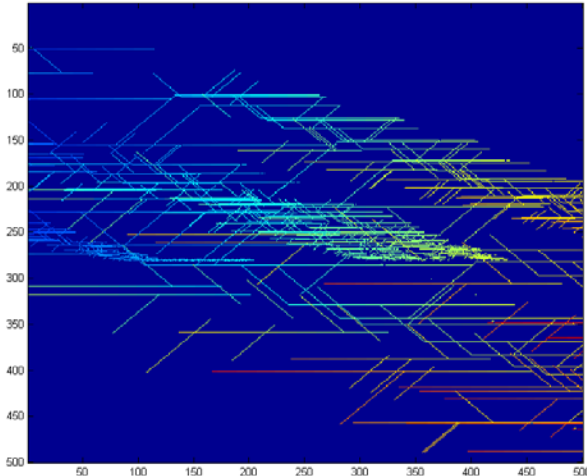


Figure 8: Final "Linear Fractal Fracture" model

For the second fractal-based fracture model, we used a Julia set. The multipliers are adjusted to achieve a realistic-looking singular fracture.

$$c = -1.408 + 0.1 * i \quad (1)$$

$$Z = x * i + y \quad (2)$$

$$Q = Z^2 + c \quad (3)$$

$$W = e^{-|Q|} \quad (4)$$

W value is calculated for each (x,y) couple.

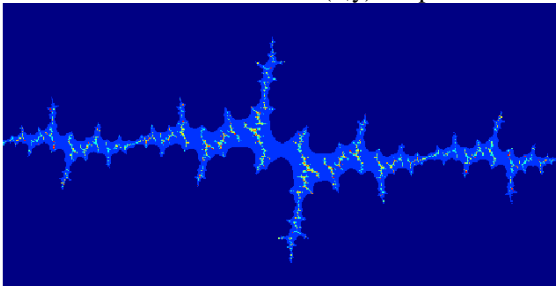


Figure 9: An individual fracture from a Julia set

This individual fracture is then placed many times in a random basis to have a fracture set.

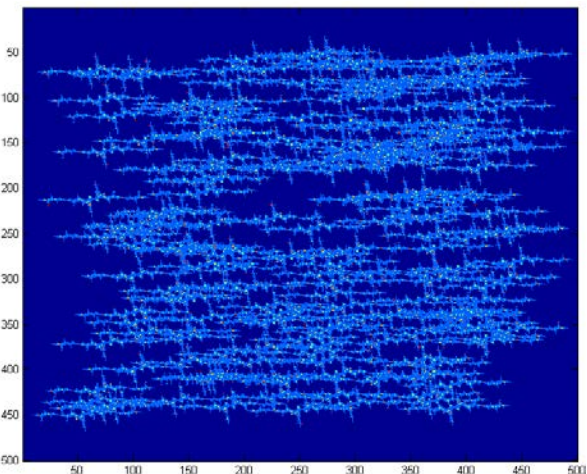


Figure 10: Final distributed Julia set fractures

1.3 Organic Material Distribution Model

Like all sedimentary rocks shales deposit with dead-organisms buried within them. While the organic matters are the reason of hydrocarbon generation, their frameworks serve as the storage units (Wang & Reed, 2009). In typical shale, total organic content (TOC) is around 10% in volume; this corresponds to 5% in weight (Wang & Reed, 2009). Organics are distributed randomly throughout the whole reservoir with a total volumetric percentage of 8 for this study.

1.4 Superposed Fracture and Organics Layers

Organics and fracture layers are superposed and the non-touched grid blocks represent the inorganic matrix. In these three base reservoir models total fracture grids and total organic matter percentages are the same. Permeability values for matrix are selected as 100 nD in x-direction and y-direction, according to [1]. Porosity values for organics are selected 60% according to [4].

Table 1: Used reservoir properties

	Organics	Matrix	Fractures
ϕ	0.6	0.04	1.0
K_x	200 mD	100 nD	500 mD
K_y	200 mD	100 nD	500 mD

Total porosity value including organics, matrix and fracture porosities are between 6%-7% (Wang & Reed, 2009). Although, to represent shale heterogeneity, smaller grid blocks are better, 1 ft per grid dimension is selected due to reservoir response results which will be used for comparison purposes only, and bigger dimensions requires less CPU time. The domains are composed of 500*500*1 grid blocks. Reservoir is set to produce to the limiting bottom-hole pressure value of 500 psia, and the initial pressure value is 5000 psia. Pressure drops are estimated and recorded for every 100 minutes for 70 days.

1.5 Homogenized Models

A bunch of homogenized reservoir models are prepared with every grid block having the same constant porosity and permeability. Porosity value is calculated from the three base models by weighted averages of different sub-elements. On the other hand, every model has a different value of permeability ranging from 1000 μ D to 500 mD. Every model with different permeability will be then compared with three previously generated models to select the best representative one.

$$\phi_h = \frac{N_f * \phi_f + N_o * \phi_o + N_m * \phi_m}{N_T} \quad (5)$$

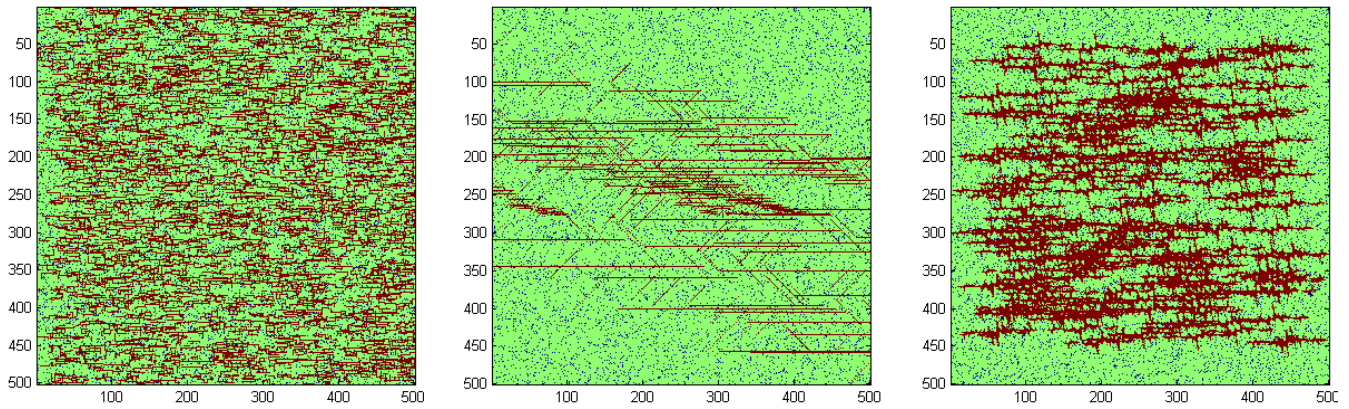


Figure 11: Fracture sets are reduced to one color. Red lines are fractures; blue dots are organics and green background is the inorganic shale matrix.

2 Results

A new comparison method is also being proposed in this paper as stated in “Methodology” section.

The homogenized and base model surfaces intersect at 14th homogenized model for the 1st base model (**Figure 12**); and at 13th for the other two base models (**Figure 13**) (**Figure 14**). 14th and 13th homogenized models have permeability values of 621 μD and 452 μD . We conclude that this reservoir can be represented with a single permeability value ranged in 450-620 μD .

Comparison between cumulative production rate of 3 base and 2 homogenized models are also given (**Figure 15**). Although there are minor differences, all models produces nearly the same amount of hydrocarbon after 70 days of production simulation.

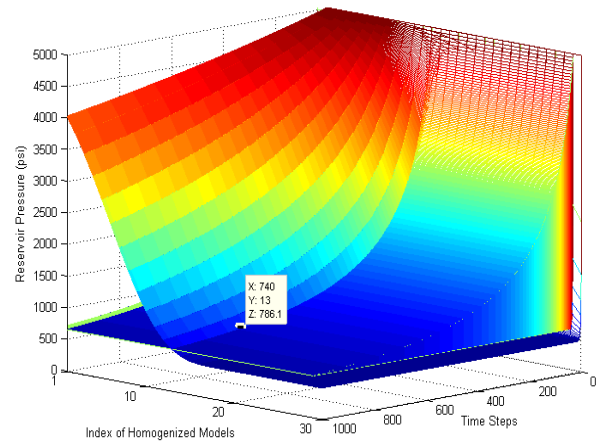


Figure 13: 2 different surfaces, one is from 2nd base model and other is from homogenized models

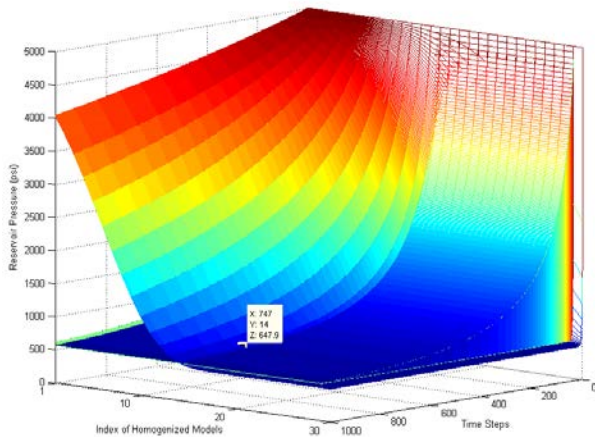


Figure 12: 2 different surfaces, one is from 1st base model and other is from homogenized models

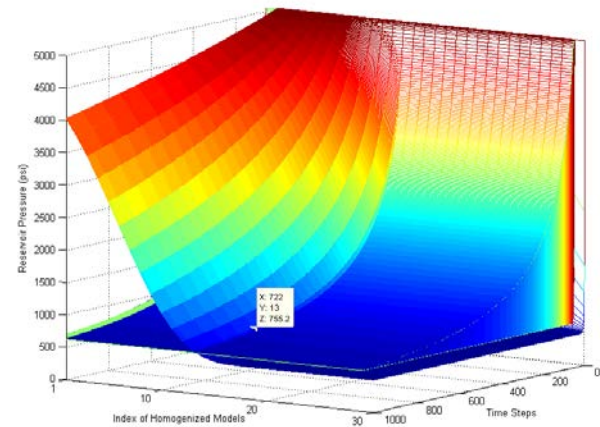


Figure 14: 2 different surfaces, one is from 3rd base model and other is from homogenized models

CONCLUSIONS

Even though all the models have the same overall number for fracture and organics grid, their distribution causes a difference and we successfully obtained an upscaled permeability value range to represent such complex reservoirs. Further steps can be applied by taking the whole upscaled reservoir as a single grid

block, with the upscaled permeability and porosity, adjacent to other grid blocks which have been undergone similar processes.

Although the focus of this study is on hydrocarbon reservoirs, other kind of earth materials, as stated in the introduction and also other lab materials are candidates for this method. The only think needed is to create representative fracture network and property design.

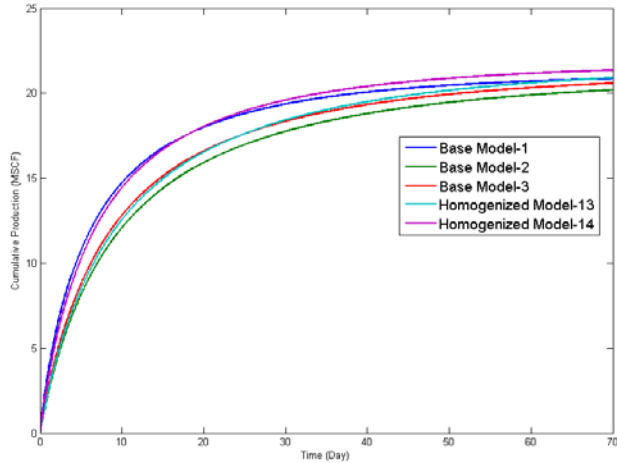


Figure 15: Comparison between cumulative production rate of 3 base and 2 homogenized models

REFERENCES

- [1] Anderson DM, Nobakht M, Moghadam S, Mattar L (2010) SPE 131787 Analysis of Production Data from Fractured Shale Gas Wells. (February), 23–25.
- [2] Gale JFW, Reed RM, Holder J (2007). Natural fractures in the Barnett Shale and their importance for hydraulic fracture treatments. *AAPG Bulletin*, 91(4), 603–622. doi:10.1306/11010606061
- [3] Nelson RA (2001) *Geological Analysis of Naturally Fractured Reservoirs* (2nd Edition).
- [4] Wang FP, Reed RM (2009) SPE 124253 Pore Networks and Fluid Flow in Gas Shales.